Chemistry & Biology 13, 1287–1295, December 2006  DOI 10.1016/j.chembiol.2006.10.005

# RNA-Mediated Sequestration of the RNA Helicase eIF4A by Pateamine A Inhibits Translation Initiation

**Marie-Eve Bordeleau,[1] Regina Cencic,[1] Lisa Lindqvist,[1] Monika Oberer,[3] Peter Northcote,[4] Gerhard Wagner,[3] and Jerry Pelletier[1,2,*]**

[1]Department of Biochemistry
[2]McGill Cancer Center
McGill University
McIntyre Medical Sciences Building
3655 Promenade Sir William Osler
Montreal, Quebec H3G 1Y6
Canada
[3]Department of Biological Chemistry and Molecular Pharmacology
Harvard Medical School
Boston, Massachusetts 02115
[4]School of Chemical and Physical Sciences
Victoria University of Wellington
Wellington
New Zealand

## Summary

**Eukaryotic initiation factor 4A (eIF4A) is a member of the DEAD-box family of putative RNA helicases whose members are involved in many aspects of RNA metabolism. eIF4A is thought to facilitate binding of 43S preinitiation complexes to mRNAs by unwinding secondary structures present in the 5′ untranslated region. Pateamine A, a small-molecule inhibitor of translation initiation, acts in an unusual manner by stimulating eIF4A activity. Herein, we report the elucidation of pateamine's mode of action. We demonstrate that Pateamine A is a chemical inducer of dimerization that forces an engagement between eIF4A and RNA and prevents eIF4A from participating in the ribosome-recruitment step of translation initiation.**

## Introduction

The ribosome-recruitment phase of translation initiation in eukaryotes is the rate-limiting step of protein synthesis and a major site of translational control. Eukaryotic initiation factor 4F (eIF4F) plays a critical role in this process and consists of three subunits: eIF4E, a protein that binds mRNA cap structures ($m^7$GpppN, where N is any nucleotide) present at the 5′ end of cellular cytoplasmic mRNAs; eIF4A, an ATP-dependent RNA helicase; and eIF4G, a scaffolding protein that recruits 43S preinitiation complexes through interactions with eIF3. eIF4F is positioned at the 5′ end of mRNAs by eIF4E, where the eIF4A subunit is thought to unwind the local mRNA secondary structure to facilitate ribosome binding [1].

eIF4A is a member of the DEAD-box protein family of putative RNA helicases. It exhibits ATP-stimulated RNA binding, RNA-dependent ATPase, and helicase activities [2]. eIF4A can exist as a free form ($eIF4A_f$) and as a subunit of eIF4F ($eIF4A_c$), and it is thought to recycle through the eIF4F complex during translation initiation [3, 4]. $eIF4A_f$ is incorporated into the eIF4F complex via its interaction with eIF4G, which contains two eIF4A-binding sites [5–8]. One site is located in the middle domain of eIF4G and is believed to stabilize RNA binding to eIF4A [9], whereas the other is present within the C-terminal domain of eIF4G and is thought to play a modulatory role in translation [5–8, 10]. eIF4G was hypothesized to act as a clamp that stabilizes the closed "active" conformation of eIF4A [11]. This is consistent with the observation that the helicase activity of $eIF4A_c$ is ~20-fold more efficient than that of $eIF4A_f$, and that the middle domain of eIF4G is capable of stimulating eIF4A ATPase activity [9, 12, 13].

The related RNA-binding proteins, eIF4B and eIF4H, also modulate eIF4A activity by increasing its RNA-binding affinity [2, 14]. eIF4B possesses an RNA recognition motif (RRM) in its N-terminal domain and an arginine-rich domain at its C terminus [15, 16]. The RRM can bind 18S rRNA, while the arginine-rich domain binds RNA in a non-sequence-dependent fashion [17]. The mechanistic details of how eIF4B affects eIF4A RNA-binding activity have not been characterized, but it appears that both RNA-binding domains of eIF4B are required [15]. A direct interaction between eIF4A and eIF4B has not been previously reported [15], although interaction between eIF4H and eIF4A has been documented [18] (A. Marintchev and G.W., unpublished data).

Pateamine A (PatA) is a small-molecule modulator of eIF4A activity recently identified as a potent inhibitor of translation [19, 20] (Figure 1A). PatA stimulates eIF4A-associated activities, but the mechanism by which it inhibits protein synthesis is not well understood. Low et al. [20] reported that this compound promotes an association between eIF4A and eIF4B, although affinity chromatography experiments with immobilized PatA have documented retention of only eIF4A, and not of eIF4B [19]. In an attempt to clarify PatA's mechanism of action, we examined its effects on association between eIF4A and eIF4B, eIF4B and RNA, and eIF4A and eIF4G. We found that eIF4A and eIF4B do not directly associate in the presence of PatA, but rather that the apparent interaction between eIF4A and eIF4B in the presence of PatA is indirect and RNA dependent. Our results indicate that PatA inhibits translation by causing eIF4A to be sequestered on RNA, thus limiting its availability for incorporation into the eIF4F complex. To our knowledge, PatA is the first example of a chemical inducer of dimerization that forces an engagement between a translation factor and RNA, thus preventing eIF4A from participating in translation initiation.

## Results and Discussion

### PatA Causes RNA-Dependent Copurification of eIF4A and eIF4B

We suspected that the PatA-induced association between eIF4A and eIF4B previously reported [20] might be indirectly mediated by RNA, since both proteins bind RNA and PatA stimulates eIF4A RNA-binding

*Correspondence: jerry.pelletier@mcgill.ca

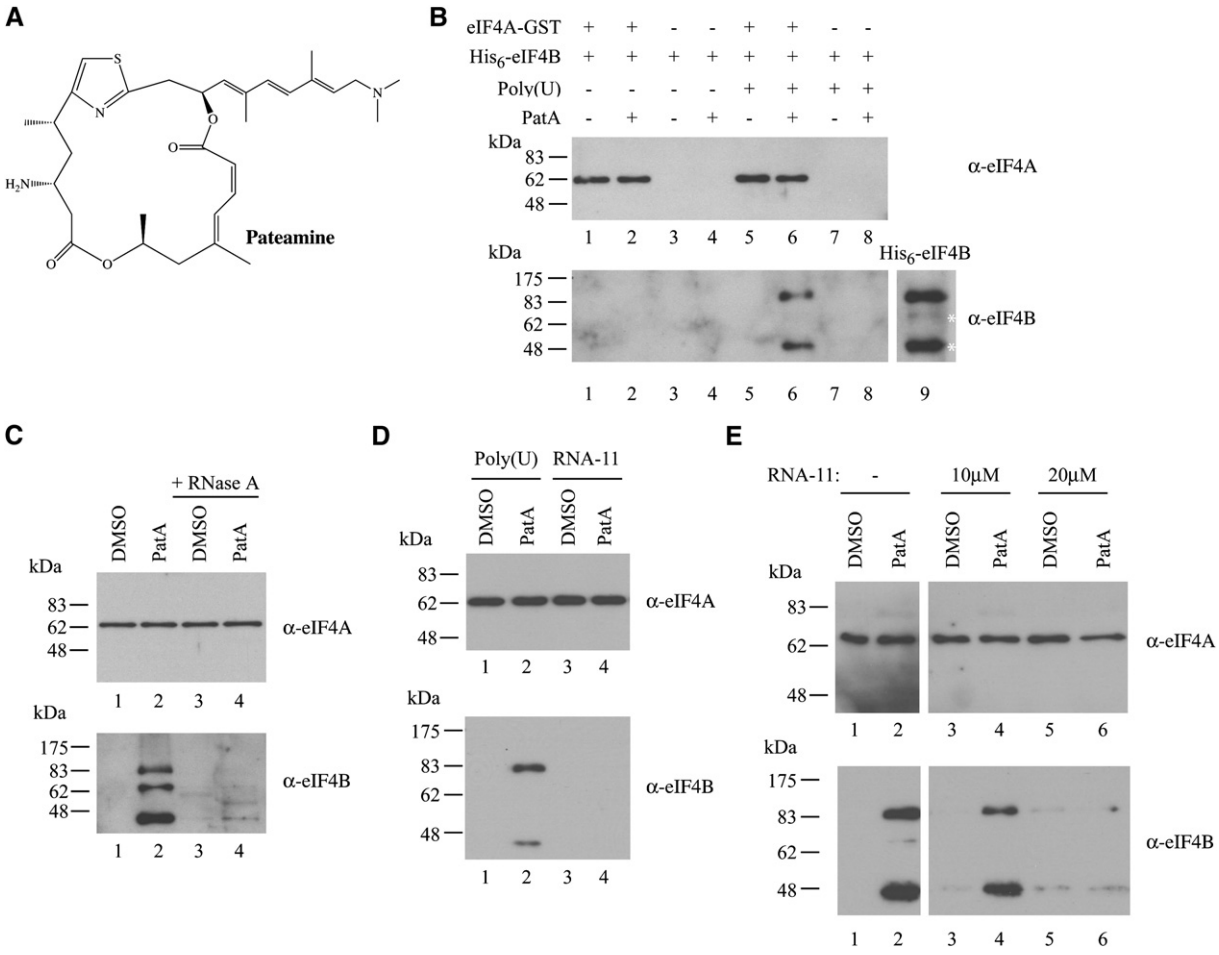


Figure 1. RNA Mediates the Association of eIF4A and eIF4B in the Presence of PatA

(A) Chemical structure of PatA.

(B) eIF4A and eIF4B copurify in the presence of PatA and RNA. $His_6$-eIF4B was incubated with eIF4A-GST in the presence of 0.5% DMSO (lanes 1, 3, 5, and 7) or 10 μM PatA (lanes 2, 4, 6, and 8). Poly(U) RNA was added where indicated. eIF4A-GST was purified using glutathione beads, and eluted proteins were subjected to SDS-PAGE and probed by western blotting using α-eIF4A (top panel) and α-eIF4B (bottom panel) antibodies. Lane 9 (bottom panel) illustrates the quality of the input recombinant eIF4B preparation used in this experiment; asterisks denote degradation products.

(C) RNase A treatment abolishes PatA-induced eIF4A:eIF4B copurification. Recombinant $His_6$-eIF4B was incubated with eIF4A-GST in the presence of poly(U) RNA and either 0.5% DMSO (lanes 1 and 3) or 10 μM PatA (lanes 2 and 4). RNase A was added where indicated (lanes 3 and 4). Complexes were purified, and proteins were resolved and visualized as described in (A).

(D) The RNA-mediated association of eIF4B and eIF4A in the presence of PatA is RNA length dependent. $His_6$-eIF4B was incubated with eIF4A-GST in the presence of 0.5% DMSO (lanes 1 and 3) or 10 μM PatA (lanes 2 and 4) and either poly(U) RNA (lanes 1 and 2) or RNA-11 (lanes 3 and 4). Complexes were purified, and proteins were resolved and visualized as described in (A).

(E) Competition by RNA-11 eliminates copurification of eIF4A and eIF4B in the presence of PatA and poly(U). $His_6$-eIF4B was incubated with eIF4A-GST in the presence of poly(U) RNA, 0.5% DMSO or 10 μM PatA, and the indicated concentrations of RNA-11. Complexes were purified, and proteins were resolved and visualized as described in (A).

activity [19]. To experimentally address this, we performed GST affinity capture experiments with purified recombinant proteins in which eIF4A-GST, $His_6$-eIF4B, and poly(U) were incubated in the presence or absence of PatA (Figure 1). The resulting complexes were then purified using glutathione beads and characterized by western blotting. An interaction between eIF4A-GST and $His_6$-eIF4B was not detected in the presence or absence of PatA when RNA was omitted from the binding reactions (Figure 1B, lanes 1 and 2). PatA caused $His_6$-eIF4B to copurify with eIF4A-GST only when poly(U) RNA was present (Figure 1B, compare lane 6 to lane 5). $His_6$-eIF4B did not associate nonspecifically with the glutathione resin, either in the absence (Figure 1B, lanes 3 and 4) or presence (Figure 1B, lanes 7 and 8) of RNA. These results suggest that the PatA-induced association between eIF4A-GST and $His_6$-eIF4B is RNA mediated. This was confirmed by the addition of RNase A to binding reactions prior to affinity capture, which abrogated copurification of eIF4A-GST and $His_6$-eIF4B (Figure 1C, compare lanes 3 and 4 to lanes 1 and 2).

We tested different RNA species for their ability to mediate PatA's effect and found that whereas poly(U) RNA (200 nucleotides long, on average [M.-E.B., unpublished data]) was able to support copurification of eIF4A-GST and $His_6$-eIF4B in the presence of PatA, an 11 nucleotide long RNA (termed RNA-11) could not (Figure 1D, compare lanes 1 and 2 to lanes 3 and 4). Preincubation of

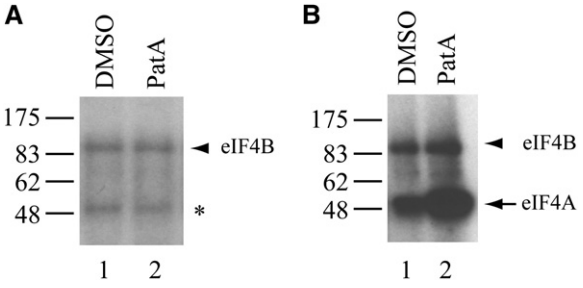


Figure 2. Assessing the Consequences of PatA on the RNA-Binding Activity of eIF4B

(A) PatA does not stimulate crosslinking of eIF4B to $^{32}$P-labeled mRNA. eIF4B was crosslinked to $^{32}$P cap-labeled β-globin mRNA in the presence of 0.5% DMSO (lane 1) or 10 μM PatA (lane 2). After nuclease digestion, samples were resolved on SDS-PAGE gels that were dried and subjected to autoradiography. The asterisk denotes a degradation product in the eIF4B preparation.

(B) Crosslinking of eIF4B to RNA in the presence eIF4A and PatA. Recombinant eIF4B and eIF4A were incubated with $^{32}$P cap-labeled β-globin mRNA in the presence of 0.5% DMSO (lane 1) or 10 μM PatA (lane 2). Proteins were crosslinked to mRNA, and samples were treated with nuclease, resolved by SDS-PAGE, and visualized by autoradiography. The position of migration of eIF4B and eIF4A is denoted by an arrowhead and an arrow, respectively.

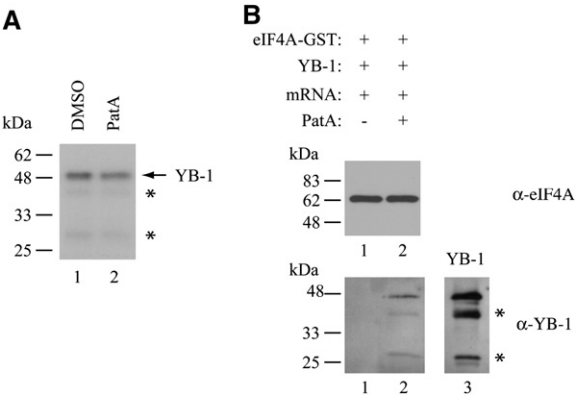


Figure 3. PatA Stimulates Copurification of eIF4A and YB-1

(A) PatA does not affect the binding of YB-1 to RNA. YB-1 was crosslinked to $^{32}$P cap-labeled β-globin mRNA in the presence of 0.5% DMSO (lane 1) or 10 μM PatA (lane 2). After nuclease digestion, samples were resolved on SDS-PAGE gels that were dried and subjected to autoradiography. Asterisks denote degradation products in the YB-1 preparation.

(B) eIF4A and YB-1 copurify in the presence of PatA and RNA. Recombinant YB-1 was incubated with eIF4A-GST and poly(A)+ mRNA in the presence of 0.5% DMSO (lane1) or 10 μM PatA (lane 2). eIF4A-GST was purified using glutathione beads, and eluted proteins were subjected to SDS-PAGE and western blotting using α-eIF4A (top panel) and α-YB-1 (bottom panel) antibodies. Lane 3 illustrates the quality of the input recombinant YB-1 preparation used in this experiment.

eIF4A-GST with RNA-11 prior to the addition of $His_6$-eIF4B and poly(U) decreased the amount of $His_6$-eIF4B copurifying with eIF4A-GST in this pull-down assay (Figure 1E, compare lanes 6 and 4 to lane 2). We rationalize that this is a consequence of RNA-11 competing out an association between eIF4A-GST or $His_6$-eIF4B and poly(U), thereby inhibiting the RNA-mediated copurification of eIF4A-GST and $His_6$-eIF4B. This suggested to us that PatA does not directly promote the binding of eIF4B to eIF4A, but rather facilitates the copurification of eIF4A and eIF4B by stimulating the ability of eIF4A to nonspecifically interact with RNA.

We have previously shown that PatA stimulates the RNA-binding activity of eIF4A in an ATP-independent fashion [19]. To determine if PatA affects eIF4B RNA-binding properties, we examined the effects of PatA on the crosslinking of $His_6$-eIF4B to mRNA (Figure 2). PatA did not significantly stimulate the binding of recombinant $His_6$-eIF4B to β-globin mRNA (Figure 2A, compare lane 2 to lane 1). Since eIF4A is known to stimulate the RNA-binding activity of eIF4B [15, 21], we monitored whether the PatA-stimulated binding of eIF4A to RNA would exert an effect on eIF4B RNA-binding properties (Figure 2B). PatA caused a 5-fold increase in the amount of eIF4A crosslinking to RNA, whereas only a slight effect on eIF4B RNA-binding activity was detected (1.5-fold increase) (Figure 2B, compare lane 2 to lane 1). These data suggest that PatA does not exert a significant effect on the RNA-binding properties of recombinant eIF4B.

### PatA Causes Copurification of eIF4A and Other RNA-Binding Proteins

If the PatA-induced association between eIF4A and eIF4B is an indirect consequence of a forced engagement between eIF4A and RNA caused by PatA, then PatA should facilitate copurification of other RNA-binding proteins with eIF4A in the presence of RNA. We therefore performed GST affinity capture experiments with eIF4A and YB-1, a nucleic acid-binding protein that is a major structural component of mRNP complexes and also a regulator of translation [22]. We first tested if PatA is able to alter the ability of YB-1 to bind RNA, and we found that PatA has no effect on the RNA-binding activity of recombinant YB-1 (Figure 3A, compare lane 2 to lane 1). We then performed GST affinity capture experiments with eIF4A-GST and YB-1 and observed that PatA facilitates copurification of YB-1 and eIF4A in the presence of poly(A)+ mRNA (Figure 3B, compare lane 2 to lane 1). The ability of PatA to mediate RNA-dependent copurification of eIF4A with other RNA-binding proteins is consistent with our previous observation that PatA stimulates the RNA-binding activity of eIF4A [19].

### PatA Inhibits 48S Complex Formation and the Incorporation of eIF4A into the eIF4F Complex

We previously reported that PatA inhibits 48S complex formation on a CAT reporter mRNA [19]. In contrast, it has been shown that PatA does not inhibit 48S complex formation but causes stalling of 48S initiation complexes on globin mRNA [20]. Given that different mRNAs were used in the two studies, and that variations in the amount of secondary structure in the 5′UTR of mRNAs are known to alter eIF4A dependency for translation [23], we assessed the effect of PatA on initiation complex formation on β-globin mRNA. Similarly to what we previously observed for CAT mRNA [19], PatA inhibited 48S complex formation on β-globin mRNA at 10 μM (Figure 4A). The reasons for the discrepancy between the two studies is not immediately apparent but may relate to the fact that our PatA preparation was isolated from the Mycale sponge [19], whereas the one used by Low et al. was of

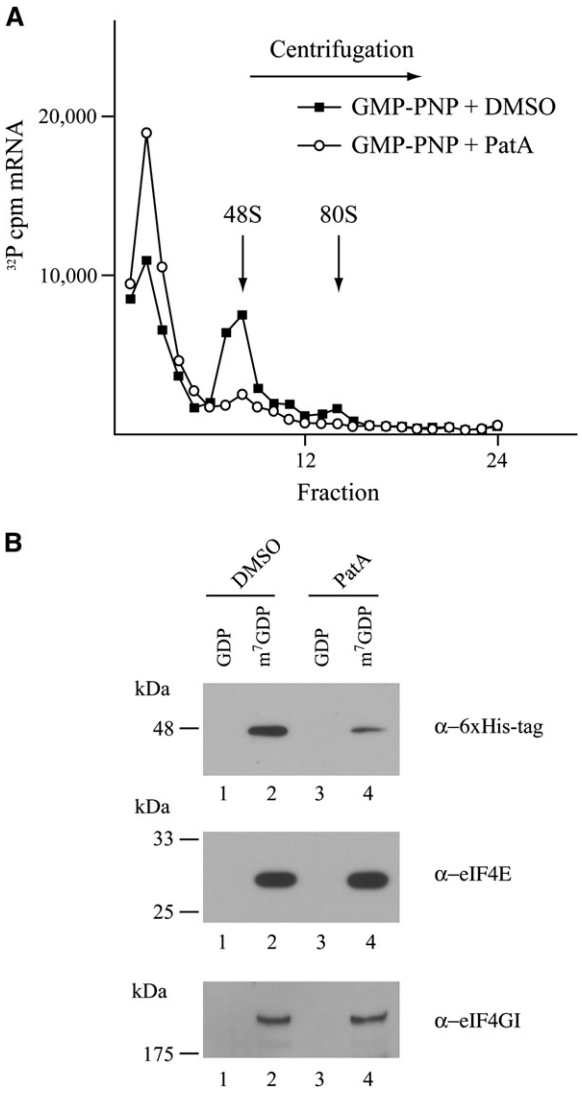


Figure 4. PatA Inhibits 48S Complex Formation on β-Globin mRNA and Incorporation of eIF4A in the eIF4F Complex

(A) PatA inhibits 48S initiation complex formation on β-globin mRNA. $^{32}$P-labeled β-globin mRNA was incubated in rabbit reticulocyte lysate containing 1 mM GMP-PNP and either 0.5% DMSO or 10 μM PatA. Reactions were resolved on sucrose gradients. After centrifugation, fractions from each gradient were collected and individually counted. Total counts recovered from each gradient and the percent mRNA bound in 48S complexes were: GMP-PNP + DMSO, 61,913 cpm, 17% binding; and GMP-PNP + PatA, 62,064 cpm, 2% binding.

(B) PatA inhibits the incorporation of eIF4A into the eIF4F complex. Initiation factor preparations were supplemented with recombinant $His_6$-eIF4A and were incubated with 0.5% DMSO or 10 μM PatA. eIF4F was purified by m$^7$GTP chromatography. The GDP and m$^7$GDP eluents were probed by western blotting for the presence of recombinant $His_6$-eIF4A, endogenous eIF4E, and eIF4GI.

synthetic origin [20]. Our results are consistent with in vitro reconstitution experiments demonstrating that eIF4A is indispensable for ribosome loading onto mRNAs containing even a modest amount of secondary structure [24].

We next addressed whether the ability of PatA to stimulate the RNA-binding activity of eIF4A could cause a reduction in the amount of eIF4A available to assemble into the eIF4F complex. This could provide an explanation for the observed decrease in 48S complex formation noted above. We therefore performed m$^7$GTP affinity capture experiments in which recombinant $His_6$-eIF4A was incubated with initiation factor preparations (ribosomal high-salt wash) in the presence or absence of PatA. Incorporation of $His_6$-eIF4A into the eIF4F complex was monitored by purifying the complexes on an m$^7$GTP affinity resin and analyzing the GDP and m$^7$GDP eluents for the presence of eIF4E, $His_6$-eIF4A, and eIF4G (Figure 4B). PatA caused a reduction in the amount of $His_6$-eIF4A associated with eIF4F, whereas eIF4E or eIF4G levels were not affected (Figure 4B, compare lane 4 to lane 2). These results are consistent with those of Low et al. [20], who documented reduced levels of eIF4AI in the eIF4F complex in the presence of PatA.

### PatA Induces RNA-Mediated Sequestration of eIF4A from eIF4G

The observation that PatA reduces the amount of eIF4A in the eIF4F complex suggests that it may directly interfere with binding of eIF4A to eIF4G. We therefore assessed if PatA inhibits the eIF4A:eIF4G interaction by performing GST affinity capture experiments with $His_6$-eIF4A and two GST-tagged eIF4GI fragments spanning the individual eIF4A-binding sites (Figure 5A) [5–8]. PatA did not inhibit the association of eIF4A with either eIF4GI$_{688–1023}$ or eIF4GI$_{1203–1600}$ (Figure 5B, compare lane 3 to lane 2 and lane 6 to lane 5). No eIF4A was retained on the glutathione resin in the absence of either GST-eIF4GI fragment (Figure 5B, lanes 1 and 4). To confirm these results, we used an independent time-resolved fluorescence resonance energy transfer assay that monitors the eIF4AI:eIF4GI interaction in a homogenous format (Figure 5C). The signal-to-background (S/B) ratio in this assay indicates that PatA neither significantly inhibits nor stimulates the interaction between $His_6$-eIF4A and either GST-eIF4GI$_{688–1023}$ or GST-eIF4GI$_{1203–1600}$ (Figure 5C). Although, eIF4GI and eIF4GII are only 46% similar, they contain homologous protein-binding domains and interact with the same factor set to form functional eIF4F complexes [25]. We therefore tested whether the interaction between eIF4GII and eIF4AI is affected by PatA (Figure 5D). In this analysis, addition of PatA to the middle domain of eIF4GII (eIF4GII-m, residues 745–1003) did not cause a change in NMR chemical shifts on uniformly labeled eIF4GII-m (Figure 5D, left panel). Addition of eIF4AI to eIF4GII-m showed substantial chemical shift changes for resonance signals of eIF4GII-m that were unaltered by the presence of PatA, indicating that PatA does not cause the eIF4GII-m:eIF4AI complex to dissociate (Figure 5D, right panel).

Our previous inability to detect copurification of eIF4E and eIF4G with eIF4A on a PatA affinity matrix indicates that only eIF4A$_f$ is bound by PatA [19] (M.-E.B., unpublished data). This suggests a model whereby PatA stimulates the non-sequence-dependent binding of eIF4A to mRNA, causing a global reduction in eIF4A$_f$ levels available for incorporation into the eIF4F complex. One prediction from this model is that eIF4G should not copurify with eIF4A when eIF4A is induced to bind RNA

in the presence of PatA. To experimentally address this, we performed affinity capture experiments in which $His_6$-eIF4A and GST-eIF4GI fragments were incubated with or without PatA in the presence of poly(U) Sepharose. In the absence of $His_6$-eIF4A, GST-eIF4$GI_{688–1023}$ was retained on the poly(U) beads (Figure 6A, bottom panel, lanes 1 and 2), an occurrence that is likely a consequence of this fragment harboring an RNA-binding site (see Figure 5A), whereas GST-eIF4$G_{1203–1600}$ was not, due to the lack of an RNA-binding motif (Figure 6A, bottom panel, lanes 5 and 6). Some $His_6$-eIF4A was pulled down by the poly(U) beads, and a concomitant increase in the amount of GST-eIF4$GI_{688–1023}$ or GST-eIF4$GI_{1203–1600}$ copurifying was noted (Figure 6A, bottom panel, compare lanes 3 and 7 to lanes 1 and 5, respectively). PatA stimulated the binding of $His_6$-eIF4A to the poly(U) affinity resin without causing an equivalent increase in the amount of GST-eIF4$GI_{688–1023}$ or GST-eIF4$GI_{1203–1600}$ being captured (Figure 6A, compare lane 4 to lane 3 and lane 8 to lane 7). These results suggest that PatA does not cause sequestration of eIF4G with RNA-bound eIF4A.

We next assessed whether PatA could cause a similar sequestration of eIF4A in vivo. We exposed cells to PatA and observed a disruption of polysomes, as previously reported (Figure 6B) [19]. We then probed fractions from the polysome gradients to determine the extent of sedimentation of eIF4A, eIF4E, and eIF4GI (Figure 6C). PatA caused eIF4A to cosediment into heavier complexes, consistent with PatA stimulating the RNA binding activity of eIF4A. To demonstrate that the change in the eIF4A sedimentation profile in the presence of PatA was mediated by the stimulation of eIF4A RNA-binding activity, we treated an aliquot of the cell extract prepared from PatA-exposed cells with nuclease prior to centrifugation (Figure 6B). This caused eIF4A to be released from heavier sedimenting complexes and regain a sedimentation profile similar to that observed with extracts prepared from untreated cells (Figure 6C). The sedimentation profile of eIF4E and eIF4GI remained unchanged in the presence or absence of PatA, consistent with our proposal that eIF4F complexes are not sequestered by RNA-bound eIF4A.

Although eIF4A is very abundant (three copies/ribosome) [26], its delivery to mRNA is mediated by eIF4F [3, 4], providing a mechanism that ensures coupling of RNA unwinding with ribosome recruitment. The results presented here suggest a model whereby RNA mediates PatA's inhibition of translation by titrating eIF4A away from the translation apparatus, rendering it unavailable to participate in the initiation phase (Figure 7). This would reduce the levels of eIF4A available for recycling into the eIF4E:eIF4G complex (Figure 7). eIF4F complexes devoid of eIF4A cannot recruit 43S preinitiation complexes on mRNAs [12, 24], thereby imposing a block at the initiation level. The regulation of translation initiation by non-sequence-selective sequestration of eIF4A (and PABP) to a small brain-specific noncoding RNA, BC1, at synaptodendritic microdomains is a well-described mechanism for repressing translation [27, 28]. To our knowledge, our results define a novel mechanism by which translation initiation is targeted by a small molecule acting as a chemical inducer of dimerization that forces the engagement between $eIF4A_f$ and RNA.

## Significance

**RNA helicases are molecular motors involved in virtually all aspects of RNA metabolism. The DEAD-box putative RNA helicases are defined by nine highly conserved amino acid motifs, making specific targeting of selected members a challenging pharmacological problem. Eukaryotic initiation factor 4A (eIF4A) is the prototypical member of the DEAD-box family of RNA helicases. It is thought to utilize energy derived from ATP hydrolysis to unwind the mRNA structure downstream of the 5′ cap structure, and, in conjunction with other translation factors, it prepares mRNA templates for ribosome recruitment during translation initiation. Pateamine, a natural product that selectively targets eIF4A and stimulates its RNA-binding properties, also inhibits translation initiation. Herein, we define pateamine's mode of action. Our data suggest a model whereby this natural product induces an engagement between eIF4A and RNA, rendering it unavailable to participate in the ribosome-recruitment phase of translation initiation. To our knowledge, pateamine is the first chemical inducer of dimerization that can force an interaction between an initiation factor (eIF4A) and RNA.**

## Experimental Procedures

### Plasmid Constructions

The plasmid pET3b/4A-GST was constructed as follows. The DraIII/BamHI fragment of pET3b/4A [19], corresponding to the C-terminal domain of mouse eIF4A, was amplified by PCR with oligonucleotides spanning these two sites. The oligonucleotide containing the BamHI site was designed to eliminate eIF4A's termination codon. The fragment generated was inserted in the DraIII/BamHI sites of pET3b/4A to generate pET3b/4A(−TGA). GST was amplified from pGEX-6P-1 with oligos containing BamHI sites, and the resulting GST tag was inserted in the BamHI site of pET3b/4A(−TGA), to create pET3b/4A-GST. The construction of pET($His_6$-eIF4B) has been previously reported [29]. Plasmids pMA311 and pMA312, which express GST-eIF4$GI_{688–1023}$ and GST-eIF4$GI_{1230–1600}$, respectively, were a kind gift of Dr. S. Tahara (USC-Keck School of Medicine, LA).

### Recombinant Proteins and Antibodies

$His_6$-eIF4AI, eIF4AI-GST, $His_6$-eIF4B, GST-eIF4$GI_{688–1023}$, and GST-eIF4$GI_{1203–1600}$were expressed in *E. coli* BL21 cells (Stratagene, Vancouver, BC) at 37°C up to an $OD_{600}$ of 0.8. After induction with 1 mM IPTG, cells were incubated at 30°C for an additional 3 hr before harvesting. $His_6$-eIF4A was purified by Ni-NTA agarose and Q-Sepharose chromatography. eIF4AI-GST, GST-eIF4$GI_{688–1023}$, and GST-eIF4$GI_{1203–1600}$ were purified on a glutathione column. $His_6$-eIF4B was purified by $Ni^{+2}$-NTA agarose and heparin Sepharose chromatography.

The anti-eIF4A antibody (5D3) is a monoclonal antibody kindly provided by Dr. H. Trachsel (University of Berne, Berne, Switzerland) and has been previously described [30]. The anti-eIF4B and anti-YB-1 antibodies are rabbit polyclonal antibodies kindly provided by Dr. N. Sonenberg (McGill University, Montreal, Canada) [22, 31]. The anti-6xHis antibody was purchased from GE Healthcare Bio-Sciences, Inc. (Baie d'Urfe, Quebec, Canada), the anti-eIF4E antibody was purchased from BD Biosciences (Mississauga, Ontario, Canada), the anti-eIF4GI antibody was obtained from Bethyl Laboratories, Inc. (Brockville, Ontario, Canada), and the anti-GST antibody was purchased from Santa Cruz (Santa Cruz, California).

### GST and Poly(U) Affinity Capture Experiments

For GST affinity capture experiments involving eIF4A-GST and $His_6$-eIF4B, 5 μg $His_6$-eIF4B was incubated with 1 μM poly(U) RNA or RNA-11 (5′-GCUUUACGGUG-3′) in binding buffer (20 mM HEPES [pH 7.5], 250 mM KOAc, 0.1% NP-40, 1 mM DTT) in the presence of 0.5% DMSO or 10 μM PatA in a 500 μl reaction at 4°C for

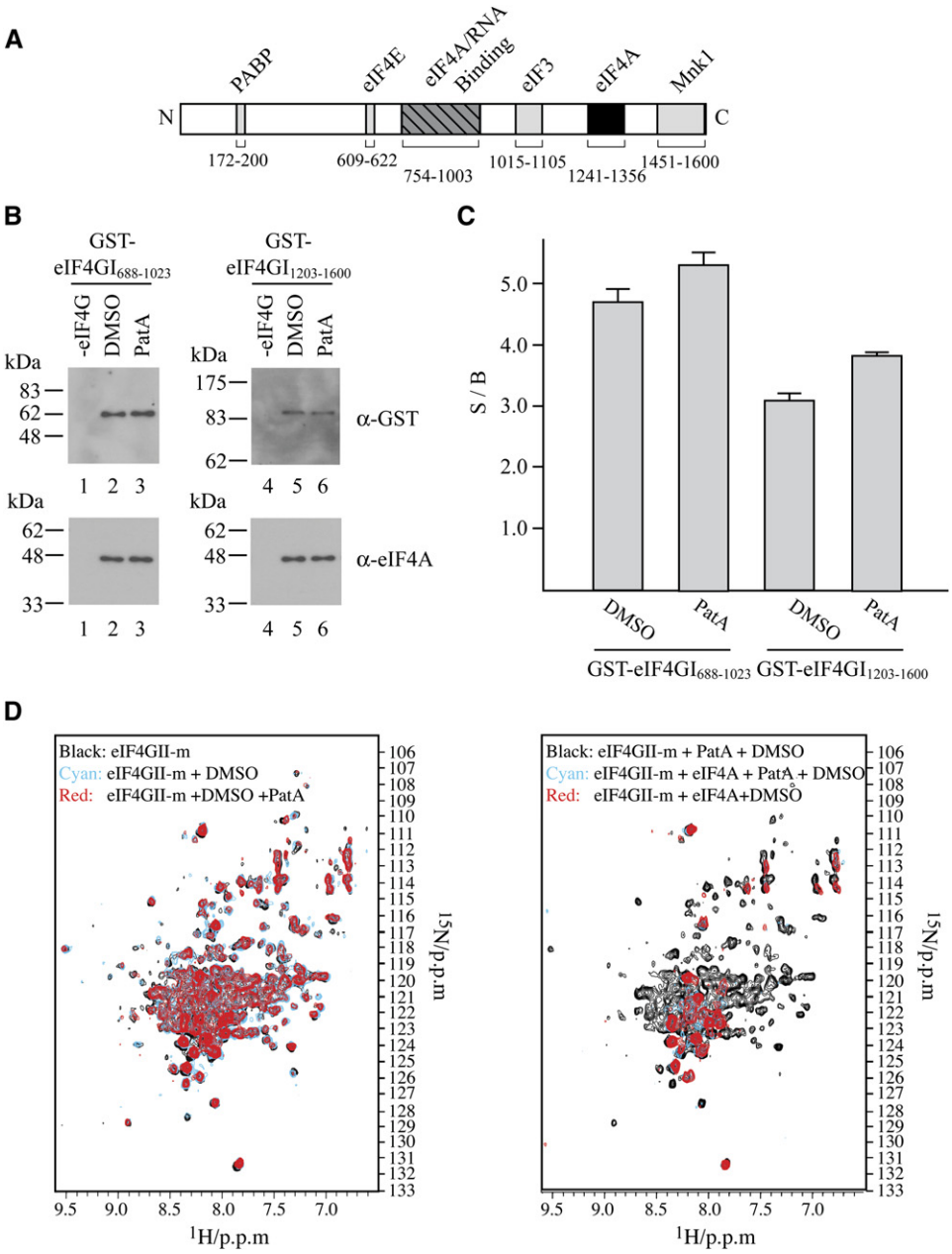


Figure 5. PatA Does Not Impair the Interaction between eIF4A and eIF4G

(A) Schematic diagram of eIF4GI. The known protein- and RNA-binding domains on eIF4GI are indicated. The numbers below eIF4GI refer to the amino acid location of each binding site.

(B) PatA does not affect the binding of eIF4A to eIF4GI. GST-eIF4GI fragments were incubated with $His_6$-eIF4A in the presence of 0.5% DMSO (lanes 2 and 5) or 10 μM PatA (lanes 3 and 6). GST-eIF4GI fragments were purified by using glutathione beads, and eluted proteins were subjected to SDS-PAGE and western blotting, using α-GST (top panel) and α-eIF4A (bottom panel) antibodies. Lanes 1 and 4 lack input GST-eIF4GI.

(C) PatA does not affect the interaction between eIF4A and eIF4GI, as assessed by time-resolved fluorescence resonance energy transfer. GST-eIF4GI fragments were incubated with $His_6$-eIF4A, as well as with Eu-W1024-labeled anti-6xHis antibody and anti-GST IgG antibody conjugated to SureLight-Allophycocyanin, in the presence of 0.5% DMSO or 10 μM PatA. The fluorescence resonance energy transfer signal was monitored on an Analyst reader (LJL Biosystems) and represents the average of four experiments; standard error of the mean is shown.

(D) PatA does not inhibit the interaction between eIF4GII and eIF4AI. Left panel: superposition of $^{1}H$-$^{15}N$-HSQC spectra of $^{15}N$-labeled eIF4GII-m (135 μM) (black); eIF4GII-m (130 μM) and DMSO (5%) (cyan); and eIF4GII-m (130 μM), PatA (130 μM), and DMSO (5%) (red). Right panel: superposition of $^{1}H$-$^{15}N$-HSQC spectra of $^{15}N$-labeled eIF4GII-m (135 μM), PatA (135 μM), and DMSO (5%) (black); eIF4GII-m (130 μM) + eIF4AI (130 μM) + PatA (130 μM) + DMSO (5%) (cyan); and eIF4GII-m (130 μM) + eIF4AI (130 μM) + DMSO (5%) (red).

10 min. A total of 0.5 μg eIF4A-GST was then added, and the incubation continued for 1 hr. Where indicated, DNase-free RNase A was added, and the reactions were incubated at 37°C for 30 min. The same procedure as that described above was followed for the GST affinity capture experiments involving eIF4A and YB-1, except that 24 μg poly(A)$^{+}$ mRNA and 18 μg YB-1 were used instead of poly(U) and eIF4B, respectively. In experiments in which eIF4A-GST was preincubated with RNA-11, the preincubation reaction

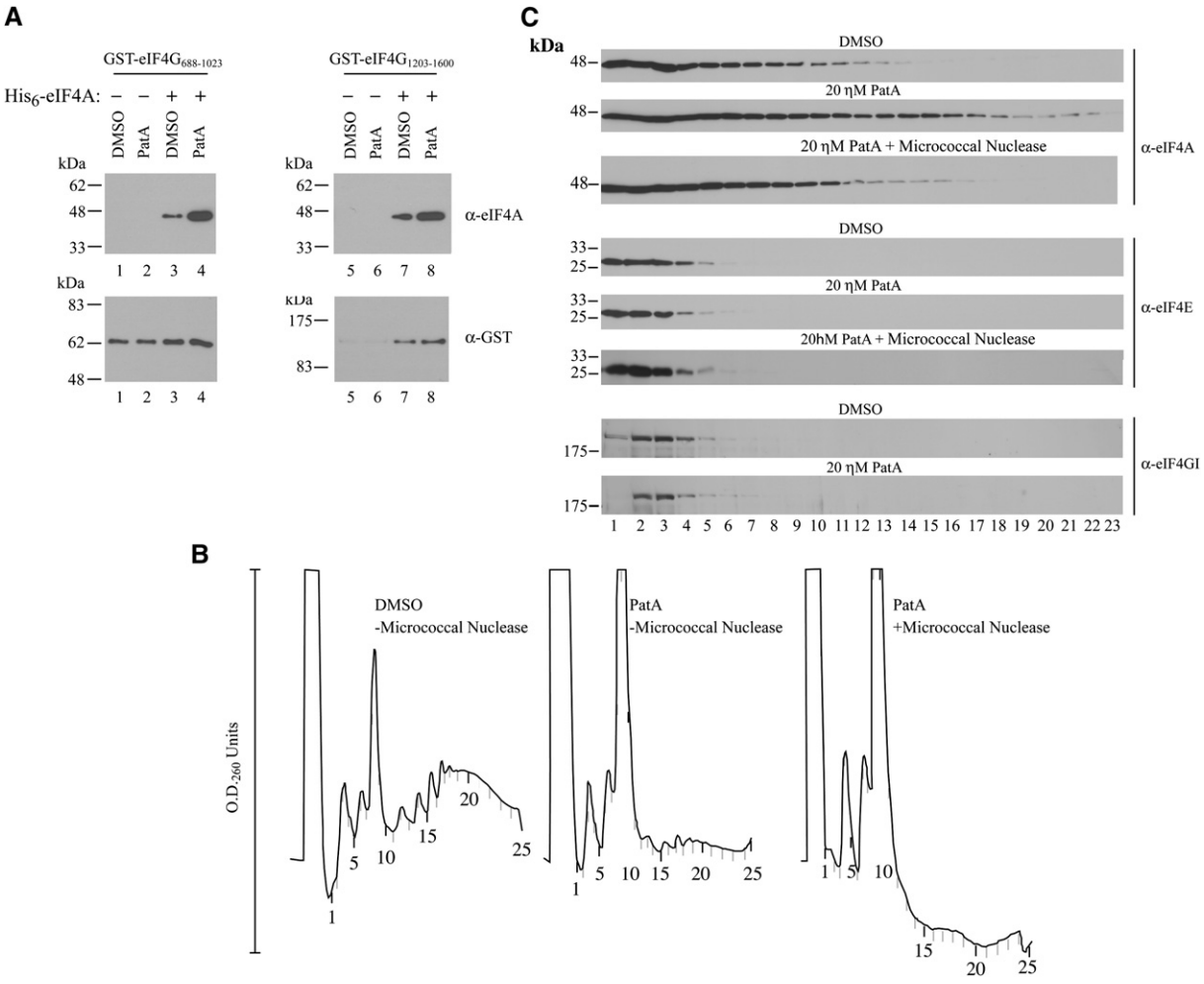


Figure 6. PatA Induces RNA-Mediated Sequestration of eIF4A from eIF4G

(A) GST-tagged eIF4GI fragments were incubated with or without $His_6$-eIF4A in the presence of 0.5% DMSO or 10 μM PatA. Pull-downs were performed with poly(U) Sepharose beads, and eluted proteins were resolved by SDS-PAGE and visualized by western blotting using α-eIF4A (top panel) and α-GST (bottom panel) antibodies.

(B) Effect of PatA on Jurkat cell polyribosomes. HeLa cells were exposed to 0.001% DMSO (vehicle) or 20 ηM pateamine for 60 min. Cellular extracts were pretreated with micrococcal nuclease where indicated. Polyribosomes were analyzed on 10%–50% sucrose gradients, and fractions were collected from the gradients.

(C) Western blots demonstrating the position of migration of eIF4A, eIF4E, and eIF4GI in fractions collected from untreated cells, cells exposed to PatA (20 ηM), and cells exposed to PatA (20 ηM) followed by micrococcal nuclease treatment (100 U/ml for 20 min at room temperature) of extracts.

was performed at 4°C for 10 min before being added to the binding reaction. All reactions were then incubated for 1 hr at 4°C with glutathione Sepharose beads. Beads were washed with binding buffer, and proteins were eluted with 10 mM reduced glutathione, resolved on 10% SDS-polyacrylamide gels, and visualized by western blotting. For GST-eIF4GI and $His_6$-eIF4A pull-down experiments, 0.5 μg GST-eIF4GI$_{688–1023}$ or GST-eIF4GI$_{1203–1600}$ was incubated with 0.2 μg $His_6$-eIF4A in binding buffer in the presence of 0.5% DMSO or 10 μM PatA in a 25 μl reaction on ice for 30 min. Complexes were purified by using glutathione beads as described above. For poly(U) affinity capture experiments, 0.5 μg GST-eIF4GI$_{688–1023}$ or GST-eIF4GI$_{1203–1600}$ was incubated with 0.2 μg $His_6$-eIF4A and poly(U) Sepharose in binding buffer in the presence of 0.5% DMSO or 10 μM PatA in a 50 μl reaction at 4°C for 1 hr. Beads were washed with binding buffer, and proteins were eluted with SDS sample buffer and were visualized by western blotting.

### Chemical Crosslinking and Ribosome Binding

Procedures for chemical crosslinking and ribosome binding are described elsewhere [32]. Ribosome bindings were performed in rabbit reticulocyte lysates with 200,000 cpm (30 ng) input mRNA. For chemical crosslinking of initiation factors to β-globin mRNA, 1 μg $His_6$-eIF4B and $His_6$-eIF4A were used. mRNA used in the ribosome-binding assay consisted of the first 200 nucleotides of β-globin, generated by in vitro transcription.

### $m^7$GTP Affinity Capture Experiments

Ribosomal salt wash was incubated with 1 μg $His_6$-eIF4A and 0.5% DMSO or 10 μM PatA at 30°C for 1 hr. A total of 60 μl $m^7$GTP-Sepharose beads was then added, and the reactions were incubated at 4°C for 2 hr. Beads were washed twice with 240 μl buffer A (20 mM HEPES [pH 7.5], 100 mM KCl, 0.2 mM EDTA) and twice with 240 μl 200 μM GDP, and proteins were eluted with 120 μl 200 μM GDP and then with 120 μl 200 μM $m^7$GDP.

### Time-Resolved Fluorescence Resonance Energy Transfer

$His_6$-eIF4A (20 ηM) and GST-eIF4GI$_{688–1023}$ (40 ηM) or $His_6$-eIF4A (100 ηM) and GST-eIF4GI$_{1203–1600}$ (200 ηM) were incubated with Eu-W1024-labeled anti-6xHis antibody (1 ηM) (Perkin Elmer, Woodbrodge, Ontario, Canada) and anti-GST IgG antibody conjugated to SureLight-Allophycocyanin (100 ηM) (Perkin Elmer, Woodbrodge, Ontario, Canada) in time-resolved fluorescence resonance energy

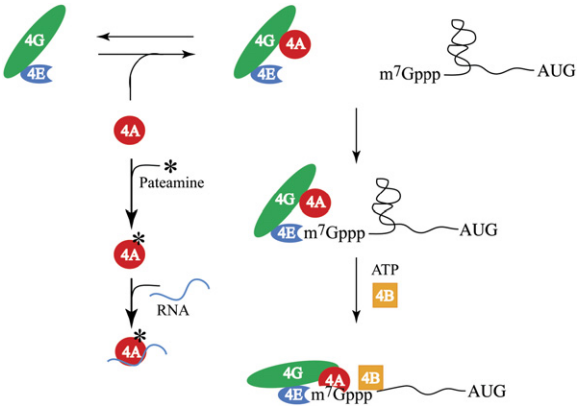


Figure 7. Proposed Model by which PatA Inhibits Translation Initiation

Sequestration of eIF4A onto RNA by PatA decreases the amount of eIF4A available for recycling through the eIF4F complex.

transfer buffer (20 mM HEPES [pH 7.4], 10 mM KCl, 1 mM DTT, 0.015% Tween 20, 1 μg/ml IgG) in the presence of 0.5% DMSO or 10 μM PatA. Reactions were performed at room temperature for 3 hr. The fluorescence resonance energy transfer signal was monitored with an Analyst HT reader (LJL Biosystems).

### NMR Spectroscopy

Expression and purification of uniformly labeled eIF4GII-m was described previously [11]. Protein was dialyzed into NMR buffer (50 mM Tris-HCl [pH 7.0], 150 mM NaCl, 5 mM DTT, 1 mM EDTA) and concentrated to 130 μM. PatA (10 mM stock solution in DMSO) was added in small aliquots to eIF4GII-m. The changes in binding after the addition of PatA and/or eIF4AI were recorded by $^{1}H$-$^{15}N$ HSQC spectra on a Varian Inova 500 MHz spectrometer equipped with a cryogenic probe.

### Polysome Profiling

Jurkat cells ($2 \times 10^{7}$) were incubated with 0.001% DMSO or 0.02 μM pateamine (dissolved in 0.001% DMSO) for 1 hr, after which the cells were collected by brief centrifugation. The cell pellets were resuspended in 500 μl lysis buffer (5 mM Tris [pH 7.5], 2.5 mM $MgCl_2$, 1.5 mM KCl, 2 mM DTT, 1% Triton X-100, 0.5% sodium deoxycholate) in the presence of 100 μg/ml cycloheximide, were vortexed, and were centrifuged briefly. Where indicated, the supernatants were treated with micrococcal nuclease as follows. Lysates were supplemented with 1 mM $CaCl_2$, 50 U micrococcal nuclease was added, and the reactions were incubated at room temperature for 20 min. The reactions were stopped by the addition of 2 mM EGTA. The lysates were loaded onto 10%–50% sucrose gradients and were centrifuged in a SW40 rotor at 35,000 rpm for 2 hr. Fractions were collected, and absorbance was monitored during the process. The fractions were then resolved on 10% SDS-PAGE gels, and proteins were visualized by western blotting with anti-eIF4A, anti-eIF4E, and anti-eIF4GI antibodies.

### Acknowledgments

We thank Dr. Francis Robert for comments on the manuscript. We are grateful to Dr. Stanley Tahara (USC, California) for his gift of GST-eIF4GI expression plasmids and to Dr. Valentina Evdokimova (UBC, Canada) for her gift of YB-1 protein. The anti-eIF4B and anti-YB-1 antibodies were kindly provided by Dr. Nahum Sonenberg (McGill University, Canada). M.O. was supported by a Max Kade Fellowship. We thank Dr. Hans Trachsel (University of Berne, Berne, Switzerland) for his kind gift of anti-eIF4A. M.-E.B. was supported by a Canadian Institutes of Health Research (CIHR) Cancer Consortium Training Grant Award and a Fonds de la recherche en santé du Québec studentship award. R.C. was supported by a CIHR Cancer Consortium Post-doctoral Training Grant Award, and L.L. was supported by a CIHR Chemical Biology Fellowship and a Maysie MacSporran studentship. This work was supported by a National Cancer Institute of Canada grant (#017099) and a National Institutes of Health grant (CA114475) to J.P.

Received: July 5, 2006
Revised: October 5, 2006
Accepted: October 17, 2006
Published: December 22, 2006

### References

1. Gingras, A.C., Raught, B., and Sonenberg, N. (1999). eIF4 initiation factors: effectors of mRNA recruitment to ribosomes and regulators of translation. Annu. Rev. Biochem. *68*, 913–963.
2. Rogers, G.W., Jr., Komar, A.A., and Merrick, W.C. (2002). eIF4A: the godfather of the DEAD box helicases. Prog. Nucleic Acid Res. Mol. Biol. *72*, 307–331.
3. Yoder-Hill, J., Pause, A., Sonenberg, N., and Merrick, W.C. (1993). The p46 subunit of eukaryotic initiation factor (eIF)-4F exchanges with eIF-4A. J. Biol. Chem. *268*, 5566–5573.
4. Pause, A., Methot, N., Svitkin, Y., Merrick, W.C., and Sonenberg, N. (1994). Dominant negative mutants of mammalian translation initiation factor eIF-4A define a critical role for eIF-4F in cap-dependent and cap-independent initiation of translation. EMBO J. *13*, 1205–1215.
5. Lamphear, B.J., Kirchweger, R., Skern, T., and Rhoads, R.E. (1995). Mapping of functional domains in eukaryotic protein synthesis initiation factor 4G (eIF4G) with picornaviral proteases. Implications for cap-dependent and cap-independent translational initiation. J. Biol. Chem. *270*, 21975–21983.
6. Imataka, H., and Sonenberg, N. (1997). Human eukaryotic translation initiation factor 4G (eIF4G) possesses two separate and independent binding sites for eIF4A. Mol. Cell. Biol. *17*, 6940–6947.
7. Korneeva, N.L., Lamphear, B.J., Hennigan, F.L., Merrick, W.C., and Rhoads, R.E. (2001). Characterization of the two eIF4A-binding sites on human eIF4G-1. J. Biol. Chem. *276*, 2872–2879.
8. Lomakin, I.B., Hellen, C.U., and Pestova, T.V. (2000). Physical association of eukaryotic initiation factor 4G (eIF4G) with eIF4A strongly enhances binding of eIF4G to the internal ribosomal entry site of encephalomyocarditis virus and is required for internal initiation of translation. Mol. Cell. Biol. *20*, 6019–6029.
9. Korneeva, N.L., First, E.A., Benoit, C.A., and Rhoads, R.E. (2005). Interaction between the NH2-terminal domain of eIF4A and the central domain of eIF4G modulates RNA-stimulated ATPase activity. J. Biol. Chem. *280*, 1872–1881.
10. Morino, S., Imataka, H., Svitkin, Y.V., Pestova, T.V., and Sonenberg, N. (2000). Eukaryotic translation initiation factor 4E (eIF4E) binding site and the middle one-third of eIF4GI constitute the core domain for cap-dependent translation, and the C-terminal one-third functions as a modulatory region. Mol. Cell. Biol. *20*, 468–477.
11. Oberer, M., Marintchev, A., and Wagner, G. (2005). Structural basis for the enhancement of eIF4A helicase activity by eIF4G. Genes Dev. *19*, 2212–2223.
12. Ray, B.K., Lawson, T.G., Kramer, J.C., Cladaras, M.H., Grifo, J.A., Abramson, R.D., Merrick, W.C., and Thach, R.E. (1985). ATP-dependent unwinding of messenger RNA structure by eukaryotic initiation factors. J. Biol. Chem. *260*, 7651–7658.
13. Rozen, F., Edery, I., Meerovitch, K., Dever, T.E., Merrick, W.C., and Sonenberg, N. (1990). Bidirectional RNA helicase activity of eucaryotic translation initiation factors 4A and 4F. Mol. Cell. Biol. *10*, 1134–1144.
14. Richter, N.J., Rogers, G.W., Jr., Hensold, J.O., and Merrick, W.C. (1999). Further biochemical and kinetic characterization of human eukaryotic initiation factor 4H. J. Biol. Chem. *274*, 35415–35424.
15. Methot, N., Pause, A., Hershey, J.W., and Sonenberg, N. (1994). The translation initiation factor eIF-4B contains an RNA-binding region that is distinct and independent from its ribonucleoprotein consensus sequence. Mol. Cell. Biol. *14*, 2307–2316.
16. Naranda, T., Strong, W.B., Menaya, J., Fabbri, B.J., and Hershey, J.W. (1994). Two structural domains of initiation factor

eIF-4B are involved in binding to RNA. J. Biol. Chem. *269*, 14465–14472.

17. Methot, N., Pickett, G., Keene, J.D., and Sonenberg, N. (1996). In vitro RNA selection identifies RNA ligands that specifically bind to eukaryotic translation initiation factor 4B: the role of the RNA remotif. RNA *2*, 38–50.
18. Feng, P., Everly, D.N., Jr., and Read, G.S. (2005). mRNA decay during herpes simplex virus (HSV) infections: protein-protein interactions involving the HSV virion host shutoff protein and translation factors eIF4H and eIF4A. J. Virol. *79*, 9651–9664.
19. Bordeleau, M.-E., Matthews, J., Wojnar, J.M., Linqvist, L., Novac, O., Jankowsky, E., Sonenberg, N., Northcote, P.T., Teesdale-Spittle, P., and Pelletier, J. (2005). Stimulation of mammalian translation initiation factor eIF4A activity by a small molecule inhibitor of eukaryotic translation. Proc. Natl. Acad. Sci. USA *102*, 10460–10465.
20. Low, W.K., Dang, Y., Schneider-Poetsch, T., Shi, Z., Choi, N.S., Merrick, W.C., Romo, D., and Liu, J.O. (2005). Inhibition of eukaryotic translation initiation by the marine natural product pateamine A. Mol. Cell *20*, 709–722.
21. Grifo, J.A., Tahara, S.M., Leis, J.P., Morgan, M.A., Shatkin, A.J., and Merrick, W.C. (1982). Characterization of eukaryotic initiation factor 4A, a protein involved in ATP-dependent binding of globin mRNA. J. Biol. Chem. *257*, 5246–5252.
22. Evdokimova, V., Ruzanov, P., Imataka, H., Raught, B., Svitkin, Y., Ovchinnikov, L.P., and Sonenberg, N. (2001). The major mRNA-associated protein YB-1 is a potent 5′ cap-dependent mRNA stabilizer. EMBO J. *20*, 5491–5502.
23. Edery, I., Lee, K.A., and Sonenberg, N. (1984). Functional characterization of eukaryotic mRNA cap binding protein complex: effects on translation of capped and naturally uncapped RNAs. Biochemistry *23*, 2456–2462.
24. Pestova, T.V., and Kolupaeva, V.G. (2002). The roles of individual eukaryotic translation initiation factors in ribosomal scanning and initiation codon selection. Genes Dev. *16*, 2906–2922.
25. Gradi, A., Imataka, H., Svitkin, Y.V., Rom, E., Raught, B., Morino, S., and Sonenberg, N. (1998). A novel functional human eukaryotic translation initiation factor 4G. Mol. Cell. Biol. *18*, 334–342.
26. Duncan, R., Milburn, S.C., and Hershey, J.W. (1987). Regulated phosphorylation and low abundance of HeLa cell initiation factor eIF-4F suggest a role in translational control. Heat shock effects on eIF-4F. J. Biol. Chem. *262*, 380–388.
27. Wang, H., Iacoangeli, A., Popp, S., Muslimov, I.A., Imataka, H., Sonenberg, N., Lomakin, I.B., and Tiedge, H. (2002). Dendritic BC1 RNA: functional role in regulation of translation initiation. J. Neurosci. *22*, 10232–10241.
28. Wang, H., Iacoangeli, A., Lin, D., Williams, K., Denman, R.B., Hellen, C.U., and Tiedge, H. (2005). Dendritic BC1 RNA in translational control mechanisms. J. Cell Biol. *171*, 811–821.
29. Pestova, T.V., Hellen, C.U., and Shatsky, I.N. (1996). Canonical eukaryotic initiation factors determine initiation of translation by internal ribosomal entry. Mol. Cell. Biol. *16*, 6859–6869.
30. Edery, I., Humbelin, M., Darveau, A., Lee, K.A., Milburn, S., Hershey, J.W., Trachsel, H., and Sonenberg, N. (1983). Involvement of eukaryotic initiation factor 4A in the cap recognition process. J. Biol. Chem. *258*, 11398–11403.
31. Methot, N., Song, M.S., and Sonenberg, N. (1996). A region rich in aspartic acid, arginine, tyrosine, and glycine (DRYG) mediates eukaryotic initiation factor 4B (eIF4B) self-association and interaction with eIF3. Mol. Cell. Biol. *16*, 5328–5334.
32. Bordeleau, M.E., Mori, A., Oberer, M., Lindqvist, L., Chard, L.S., Higa, T., Belsham, G.J., Wagner, G., Tanaka, J., and Pelletier, J. (2006). Functional characterization of IRESes by an inhibitor of the RNA helicase eIF4A. Nat. Chem. Biol. *2*, 213–220.